Quaternary Science Reviews 270 (2021) 107177

Contents lists available at ScienceDirect

Quaternary Science Reviews

journal homepage: www.elsevier.com/locate/quascirev

Early-warning signals for Cenozoic climate transitions

Christopher Boettner [a, *], Georg Klinghammer [a], Niklas Boers [a, c, d], Thomas Westerhold [e], Norbert Marwan [a, b]

[a] Potsdam Institute for Climate Impact Research, Member of the Leibniz Association, Telegrafenberg, 14473, Potsdam, Germany
[b] Institute of Geosciences, University of Potsdam, Potsdam, Germany
[c] Department of Mathematics and Computer Science, Free University of Berlin, Berlin, Germany
[d] Global Systems Institute and Department of Mathematics, University of Exeter, Exeter, UK
[e] MARUM–Center for Marine Environmental Sciences, University of Bremen, 28359, Bremen, Germany

ARTICLE INFO

Article history:
Received 27 May 2021
Received in revised form
31 August 2021
Accepted 1 September 2021
Available online 7 September 2021

Handling Editor: A. Voelker

Keywords:
Abrupt climate transitions
Critical slowing down
Early-warning signals
Cenozoic
Non-linear time series analysis

ABSTRACT

Deep-time paleoclimatic records document large-scale shifts and perturbations in Earth's climate; during the Cenozoic in particular transitions have been recorded on time scales of 10 thousand to 1 million years. Bifurcations in the leading dynamical modes could be a key element driving these events. Such bifurcation-induced critical transitions are typically preceded by characteristic early-warning signals, for example in terms of rising standard deviation and lag-one autocorrelation. These early-warning signals are generated by a widening of the underlying basin of attraction when approaching the bifurcation, a phenomenon dubbed critical slowing down. The associated dynamical transitions should therefore be preceded by characteristic signals that can be detected by statistical methods. Here, we reveal the presence of significant early-warning signals prior to several climate events within a paleoclimate record spanning the last 66 million years - the Cenozoic Era. We computed standard deviation and lag-one autocorrelation of the CENOzoic Global Reference benthic foraminifer carbon and oxygen Isotope Dataset (CENOGRID), comprising two time series of deep sea carbonate isotope variations of 18O and 13C. We find significant early-warning signals for five out of nine previously identified Cenozoic paleoclimatic events in at least one of the two records, which can be considered as viable candidates for bifurcation-induced transitions to be analysed in follow-up studies. Our results suggest that some of the major climate events of the last 66 Ma were triggered by bifurcations in leading modes of variability, indicating bifurcations could be a key component of Earth's climate system deep-time evolution.

1. Introduction

Paleoclimate records show that abrupt climate changes have occurred throughout Earth's geological history (Alley et al., 2003; Dakos et al., 2008). Such events are often associated with tipping points, i.e., critical thresholds of a time-varying control parameter that lead to sudden and potentially irreversible transitions in dynamical systems. In light of anthropogenic climate change, the mechanisms behind such tipping events have attracted substantial research interest (Lenton and Schellnhuber, 2007; Lenton et al., 2019), given their potentially severe impact on society (Xu et al., 2020). Key components of the modern climate system that may exhibit abrupt transitions in response to future anthropogenic forcing have been identified (Lenton et al., 2008). Although relatively abrupt regional climate shifts can also be identified in climate model projections (Kleinen et al., 2003; Drijfhout et al., 2015), it remains debated whether comprehensive climate models would be skilful in predicting future abrupt climate transitions (Valdes, 2011). In particular, there is room for improvement concerning the consistency between the models and the available paleoclimatic transitions, although substantial advances have been made for some abrupt climate shifts such as the millennial-scale Dansgaard-Oeschger events (Vettoretti and Peltier, 2016). Moreover, the possibility of global-scale transitions or a destabilization of the entire climate system, with runaway-warming under future CO_2 increases as suggested by Steffen et al. (2018), remains debated and has not been found in climate model simulations. A better understanding of the processes behind global-scale abrupt climate transitions in the Earth's long-term past is therefore of great importance for improving our understanding of the climate system and for our

* Corresponding author.
E-mail address: boettner@pik-potsdam.de (C. Boettner).

https://doi.org/10.1016/j.quascirev.2021.107177
0277-3791/

capability of assessing the future risk of such transitions.

Bifurcation-induced tipping is a widely studied mechanism for sudden climate transitions (Stommel, 1961; Budyko, 1969; Sellers, 1969; Ashwin et al., 1962). Importantly, transitions triggered by bifurcations are typically associated with a characteristic widening of the underlying basin of attraction of the equilibrium state on the way to the bifurcation (Scheffer et al., 2009; Kuehn, 2011). This leads to a weakening of the restoring forces to perturbations, which causes the phenomenon of Critical Slowing Down (CSD) (Dakos et al., 2008; Ditlevsen and Johnsen, 1944-8007). CSD changes the statistical properties of the system and, in particular, leads to an increase of the standard deviation and lag-one autocorrelation before the tipping point is reached. These changes are frequently referred to as statistical *Early-Warning Signals* (EWS), since they occur prior to the imminent transition. These EWS have already been identified in ecological time series, controlled biological experiments, and a multitude of model simulations of different systems (Scheffer et al., 2009; Dakos et al., 2008; El-Hacen et al., 2018). In the context of paleoclimate research, EWS are not used as a forecasting tool but as means for understanding the underlying dynamics, particularly for assessing if a climate event might be caused by a bifurcation in an underlying dynamical mode consistent with a transition in the dynamical system sense. For example, EWS prior to most of the millennial-scale, northern-hemisphere abrupt climate shifts that occurred during previous glacial intervals suggest bifurcations operating at sub-centennial time scales as underlying mechanism of these Dansgaard-Oeschger events (Rypdal, 2015; Boers, 2018). Here, we focus on EWS for global-scale climate events during the last 67 million years (Ma) on decamillennial to million-year time scales. During the Cenozoic Era, a number of abrupt climate events occurred on a wide range of time scales (Adams et al., 1999; Zachos et al., 1993), including the Paleocene/Eocene Thermal Maximum (PETM) (McInerney and Wing, 2011; Westerhold et al., 2020) on 10 thousand-year time scales and Eocene/Oligocene Transition (EOT) (Miller et al., 1987) on million-year time scales. In addition to these, the millennial-scale glacial terminations are relatively abrupt transitions that are likely paced by orbital forcing. Yet, EWS prior to several of these transitions have been identified, suggesting an interplay between self-sustained oscillations possibly triggered by recurring bifurcations and the astronomical forcing.

Changes in Cenozoic climates have been studied and categorized before (Mudelsee et al., 2014), but no analysis for critical slowing down has systematically been carried out. The recently published high-resolution CENOzoic Global Reference benthic foraminifer carbon and oxygen Isotope Dataset (CENOGRID) (Westerhold et al., 2020) enables us to systematically search for indications of CSD across the most prominent (10 thousand-year to million-year time scale) events of this era. This analysis permits an assessment if bifurcations are a viable candidate for explaining (some) Cenozoic climate transitions and provides candidates for detailed analysis in follow-up studies that focus on the specific physical mechanisms behind these bifurcations and include multiple additional (regional) paleoclimate records.

CENOGRID is a composite record spanning the past 67 million years. It has been constructed from 14 astronomically tuned deep-sea drilling core records gathered across the Earth with varying sampling resolution. In this way, CENOGRID offers a reliable stratigraphic reference of the Cenozoic global climate. The data has been collected from benthic foraminifera and encompasses the evolution of $\delta^{18}O$ and $\delta^{13}C$ isotopes from the ambient deep sea water masses. The statistical characteristics of the CENOGRID composite records are not continuous due to its composition from several different cores and varying sampling rates. Since this would bias the CSD indicators (standard deviation and lag-one autocorrelation) if not accounted for, we thoroughly process the data in a way that avoids such biases, as described in detail in the methods section below.

We split the data into three parts, Section I (66–45 Ma), Section II (45–34 Ma) and Section III (34–0 Ma). The early Section contains the Paleocene and first half of the Eocene periods, where the Earth's climate was in a hothouse and warmhouse state (Westerhold et al., 2020). The Cenozoic began with the K–Pg meteorite impact 66 Ma ago (Alvarez et al., 1980). Prominent climate events during this time are the Latest Danian Event (62.2 Ma, (Bornemann et al., 2009; Westerhold et al., 2011)) and Paleocene/Eocene Thermal Maximum (55.5 Ma, (McInerney and Wing, 2011)). Section II begins at 45 Ma, it encompasses the Late Lutetian Thermal Maximum (41.5 Ma, (Westerhold et al., 2018)) and Middle Eocene Climate Optimum (40 Ma, (Bohaty and Zachos, 2003)). At the end of Section II the transition between warmhouse and icehouse states is marked by the Eocene/Oligocene Transition (33.9 Ma, (Miller et al., 1987)). At this transition point the sampling rate of CENOGRID changes from 5 ka to 2 ka due to a change in sedimentation rate and thus sample resolution. At this point, Section III starts, spanning the Oligocene, Miocene, Pliocene, and entire Quaternary. The climate is characterized to be in coldhouse and icehouse state (Westerhold et al., 2020), with notable sudden events being the Oligocene/Miocene Transition (22.5 Ma, (Zachos et al., 1997)), middle Miocene Climate Transition (13.9 Ma, (Pearson and Palmer, 2000)), Tortonian Thermal Maximum (10.75 Ma, (Westerhold et al., 2020)), and the Late Miocene Carbon Isotope Shift (7.6 Ma, (Hodell et al., 2001)). This list of sudden events is not exhaustive, further shifts have been identified in the Cenozoic. We choose to limit our focus to these events since they are the most prominent within CENOGRID. The authors of the original publication (Westerhold et al., 2020) have performed a recurrence analysis and all these events cause characteristic changes in the recurrence pattern consistent with dynamical transitions. They are further accompanied by recognizable features in the time series data, either sudden mean changes or local extrema. All of these events can be identified in both records ($\delta^{18}O$ and $\delta^{13}C$) (with exception of the Late Miocene Carbon Isotope Shift). This enables us to check for consistency between EWS in both datasets.

We choose to analyse the events separately in each of the three parts for two reasons. For one, the data density for Section I and Section III differs greatly, which results in the resolution discrepancy mentioned before. It may be the case that time scales for the appearance of CSD vary between Sections of 5 ka and 2 ka of temporal resolution. Additionally, a case can be made that the dynamics within the warm states (hot- and warmhouse state) may differ significantly from the one in the cold states (ice- and coldhouse). Complementary, CSD may be observable on similar time scales for all events within each of the three parts of the time series. We further chose to investigate Section II separately, since this part of the data has a noticeably lower sampling rate (see Fig. 1). Our analysis of the events is therefore only possible on very short time scales and cannot be evaluated by the same means as for the other Sections.

It is possible that changes in statistical properties indistinguishable from EWS may arise either due to random fluctuations or by mechanisms unrelated to critical slowing down. Therefore, a statistical test regarding the significance of the observed signals (magnitude and number of EWS) is performed. We refer to the methods section below for details on the EWS estimation, significance test, as well as data pre-processing. EWS are searched for in terms of significant positive (linear) trends in standard deviation and lag-one autocorrelation in both CENOGRID records. The results are subdivided into the three Sections mentioned earlier. By dividing the data, we guarantee the comparability of the results within each Section, which is required for our global significance

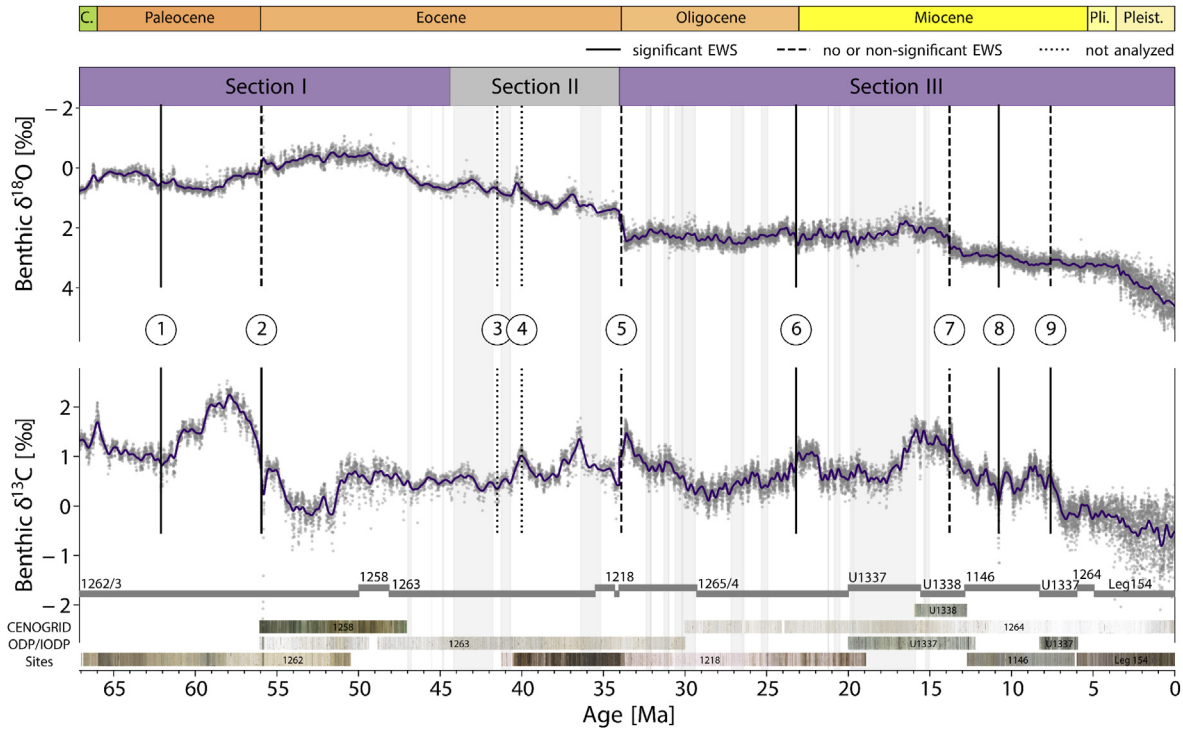

Fig. 1. The CENOGRID $\delta^{18}O$ and $\delta^{13}C$ records. The data is smoothed by a locally weighted function over 1.2Ma (Section I and II) or 755ka (Section III) (violet curve). For detrending, the smooth curve is subtracted from original data. Events are considered to be preceded by significant EWS if a locally significant increase in both σ and α_1 can be observed (CSD-like behaviour, see Methods section). For a detailed breakdown, see Table 2. Grey-shaded areas are parts of time series where data is insufficient for reliably estimating the standard deviation and autocorrelation. Data sparsity is most severe prior to events in Section II and in the interval 20 to 15 Ma. Drilling core records (see section 2.5) are marked on the bottom (grey bands) and assigned their respective ODP Site number. Below that are images of the original drilling cores that were used to create CENO The nine events (vertical lines) are in ascending order: (1) Latest Danian Event, (2) Paleocene/Eocene Thermal Maximum, (3) Late Lutetian Thermal Maximum, (4) Middle Eocene Climate Optimum, (5) Eocene/Oligocene Transition, (6) Oligocene/Miocene Transition, (7) middle Miocene Climate Transition, (8) Tortonian Thermal Maximum, and (9) Late Miocene Carbon Isotope Shift. (For interpretation of the references to colour in this figure legend, the reader is referred to the Web version of this article.)

test (see section 2.3) regarding the number of EWS. This is required since the varying resolution within the record leads to different parameters used in the EWS estimation. The results are put into context in the Discussion section, where also further research directions are outlined.

2. Methods and materials

2.1. Data preprocessing

We employ an alternative, non-interpolated version of CENOGRID for the $\delta^{18}O$ and $\delta^{13}C$ records. For this version, the raw data was first sorted into equally spaced time bins and then combined within each bin to form representative, equidistant sampling points. The original publication of CENOGRID went through further processing steps, including interpolation and smoothing, which alter the properties of the time series (Schulz and Stattegger, 1997; Schulz and Mudelsee, 2002). Employing the binned, non-interpolated data helps avoid biases in the statistical properties introduced by these steps. This binning procedure yields equidistant sampling steps of 5 ka (67–34 Ma) and 2 ka (34–0 Ma). Without interpolation, some of these bins are empty, leaving gaps in the time series. The next section details how this problem is handled.

The CSD indicators standard deviation (σ) and lag-one autocorrelation (α_1) are computed in (centred) running windows of size $w = 755$ ka and 330 ka for Section I and Section III, respectively, using the equations

$$\sigma(x) = \sqrt{\frac{1}{n}\sum_{i=1}^{n}(x_i - \overline{x})^2},$$
$$\alpha_1(x) = \frac{\sum_{i=1}^{n}(x_i - \overline{x})(x_{i-1} - \overline{x})}{\sqrt{\sum_{i=1}^{n}(x_i - \overline{x})^2}\sqrt{\sum_{i=1}^{n}(x_{i-1} - \overline{x})^2}}. \quad (1)$$

where the index i runs over all data points x_i within a given window, n denotes the amount of data points and $\overline{x}$ the arithmetic mean of all data points in the window. Prior to this step, the data has to be detrended to avoid biasing the calculation. Detrending is done using a running weighted mean with a centred Gaussian kernel with variance s_d^2 and a total bandwidth of $6s_d$. Gaussian filters work effectively as low-pass filters and since CENOGRID is sampled at two different rates (bin sizes), different values of s_d^2 are used for each Section.

When calculating the trends in the CSD indicators, special care has to be taken to not include information of the transition itself, since this could lead to spurious trends in the indicator. This means that the CSD indicator window is not allowed to cross the point of the event and the Gaussian filter window can only cross marginally. For this reason, only data up to $2s_d + 0.5w$ before the event is included into the trend calculation, with w being the window width for the σ and α_1 calculation. The window thus only includes detrended data points prior to the events.

2.2. Dealing with missing values

For all analysis, the binned, non-interpolated versions of the CENOGRID records are used. This avoids biases due to interpolation or regression, but leaves a non-equidistant time series with missing values and varying data density, due to varying sampling resolution in the original records. This is quantified by calculating the fraction of non-missing values within a window used to calculate the CSD indicator.

Since σ and α_1 need slightly different inputs, two kinds of data densities are needed. For σ estimates, the important value is the total number of data points within a window, which we call the *point density*. To calculate the lag-one autocorrelation, two neighbouring data points are needed. We call the number of these neighbouring data points the *pair density*. Both of these values vary strongly in the data, with some parts having almost 100% pair density and some with less than 10%. There are a number of possible ways how to account for missing data and non-equidistant time series. A common method is to interpolate the data to a constant sampling rate (see e.g., (Dakos et al., 2008; Boers, 2018; Trauth et al., 2019)). This can, however, introduce a bias into the CSD indicator if the underlying data density changes significantly (see Supplementary Material, figs. A.8 and A.9). Generally, a low pair density leads to an overestimate of the autocorrelation using the interpolation approach (Rehfeld et al., 2011). We chose here to ignore the missing values when calculating the estimators. That is, σ is only calculated from the actual data present within a window, and correspondingly, α_1 is calculated only from those data pairs present in a given window. The same is done for the running mean detrending. This method also influences the estimators. To be more precise, a lower density of points or pairs in a given window leads to a higher uncertainty in the σ and α_1 estimators. Tests on toy models, however, suggest the estimators are largely unbiased (see Supplementary Material, figs. A.10 and A.11), in contrast to the case of indicators computed for time series where missing values are interpolated.

We only consider data with a point density above 40% and a pair density above 20% viable for this type of analysis, since uncertainties in the estimators will mask any actual signal for lower densities (see, e.g., Fig. A.6, 20–15 Ma). For this reason, the middle Section (45–33 Ma) is analysed separately from the rest of the data. The events in this Section are preceded by intervals with a consistent point density below 40% and pair density near 0%. The resulting effect on the estimators is clearly visible in figs. A.4 and A.6 of the Supplementary Material; it is impossible to compute α_1 on some intervals prior to the transition. The interval 20–15.56 Ma is also excluded from the global significance test, due to a poor pair density near 0%.

2.3. Significance tests

Within the scope of this work, CSD-like behaviour is defined as the occurrence of EWS prior to a transition, where *EWS* is defined as a significant increase in σ and α_1 prior to a transition as demanded by CSD theory. To evaluate the significance of such trends, two statistical tests are performed, which we refer to as the local and the global test. The local test assesses the probability that the increase in the CSD indicators (windowed σ and α_1) happens by statistical fluctuations in the estimator time series, given their own statistical properties. This test is carried out for every event and every quantity separately, and is performed on the basis of random phase (RP) Fourier transform surrogates (see (Lancaster et al., 2018) for background and (Rypdal, 2015; Boers, 2018) for applications), to preserve the standard deviation and autocorrelation of the respective CSD indicator time series. Since no information about the transition is allowed to be included in the trend estimation, not all values up to the transition can be included (see 2.1). For more information on this procedure, see (Rypdal, 2015; Boers, 2018), where a similar analysis is performed.

We use 10,000 individual surrogates for each test case and consider an observed linear increase to be statistically significant if less than 5% of the surrogates show a trend comparable or larger than the original time series ($p < 0.05$). Based on the results, each event is assigned one of three categories ranking their validity as potential CSD candidate from weakest to strongest (Table 1). *Nondescript* behaviour encompasses negative results, where no noteworthy indications of CSD can be inferred from the behaviour of σ and α_1. The second category includes events where *CSD-like* behaviour can be observed in at least one of the two records, meaning a consistent increase in standard deviation and lag-one autocorrelation. The last category, *synchronized CSD-like* behaviour, comprises events where CSD-like behaviour can be consistently identified in both records prior to the events. We consider events that fall into the second and third category as valid CSD candidates. Consistent appearances of positive trends in both records reduce the probability for this behaviour to be caused by random fluctuation and thus increase its credibility as actual CSD. Yet, appearance of CSD-like behaviour in only one time series does not rule out this option since CSD might only occur in a subset of dynamical variables. Events in a stronger category also fulfil the criteria of the weaker categories.

While the local test can be used to judge the validity of the observed signal as potential sign of CSD by comparing to the expected behaviour, it does not exclude the possibility that the properties of the CENOGRID time series are such that CSD-like behaviour may happen without actual CSD occurring. For example, σ and α_1 could increase due to changes in noise properties independently of the occurrence of a critical transition in the dynamical system. We can never exclude this possibility, but we can get more confident in the results if the observed behaviour prior to events is unusual for the time series in general, meaning it rarely appears in other parts of the data. To examine this, we employ a global significance test. First, a number of points corresponding to the number of valid CSD candidates (within the Section) are chosen randomly from the time series. Then the CSD indicator preceding these points are calculated within the same intervals as their corresponding events. The behaviour prior to each random point can thus be classified in the same fashion as for the true transitions; nondescript, CSD-like, or synchronized CSD-like. Repeating this step 10,000 times creates a distribution of the number of EWS (CSD-like or synchronized CSD-like) preceding random points, against which the number of EWS preceding the actual transitions can be compared. Global significance is also declared for $p < 0.05$, meaning that in over 95% of the cases the number of EWS of the respective category preceding abrupt events could not be reproduced prior to random points. Further, the global significance of increasing standard deviation and lag-one autocorrelation individually are also globally tested to enable a better understanding of the CSD indicators' behaviour within each Section. Performing the global analysis in this fashion is the primary reason for analysis the data in different Sections independently. Since Section I and III have vastly different time resolutions, different smoothing and window parameters are required, making individual results incomparable between Sections. Additionally, low resolution in Section II makes a global significance test in this Section impossible.

2.4. Analysis intervals and parameters

Without a theoretical model for the cause of the events it is not

Table 1
Categorization of behaviour based on results obtained from local significance test. Ordered from weakest to strongest evidence for CSD.

Behaviour	Criteria
Nondescript	significant trend in no more than one indicator per time series
CSD-like	significant trends in both indicators within one time series (EWS)
synchronized CSD-like	significant trends in both indicators and in both time series

Table 2
Results of local significance test for trends calculated in the estimated CSD intervals, based on 10,000 Fourier surrogates for each case. Significant results ($p < 0.05$) are marked **bold**. For more information for the categorization, see the Methods section. Note that the timing of the event is chosen as the most likely occurrence of a dynamical transition and does not necessarily coincide with the ones commonly found in the literature.

Event	Time	δ^{13}C		δ^{18}O		Result
	[Ma]	σ	α_1	σ	α_1	
Latest Danian Event	62.1	**0.0**	**0.0**	**0.0**	**0.0**	synchr. CSD-like
PETM	55.9	**0.007**	**0.0**	0.637	**0.0**	CSD-like (δ^{13}C)
Eocene/Oligocene Transition	33.9	0.941	**0.014**	0.134	**0.001**	nondescript
Oligocene/Miocene Transition	23.2	**0.006**	**0.034**	**0.010**	**0.049**	synchr. CSD-like
middle Miocene C. Transition	13.8	0.401	**0.001**	0.953	0.139	nondescript
Tortonian Thermal Maximum	10.8	**0.0**	**0.019**	**0.004**	**0.048**	synchr. CSD-like
Late Miocene C-Isotope Shift	7.6	**0.0**	**0.0**	0.055	0.462	CSD-like (δ^{13}C)

possible to estimate the time scales on which the early-warning signals should be visible. The interval we consider to be relevant must therefore be chosen heuristically. This introduces a freedom that, if not treated carefully, could lead to false-positive results by fine-tuning the parameters. To limit this risk, a number of additional assumptions are made. CSD theory mandates that changes in autocorrelation and standard deviation should start simultaneously. We, therefore, require our analysis intervals to be the same for both estimators. Further, we demand that the intervals should be the same in both records under the assumptions that the transitions occur due to the same mechanism in both time series. Finally, we require CSD to occur on similar time scales and with the same parameters (e.g., window width) in each section. In principle, it is of course conceivable that different dynamical models affect the two variables differently and with varying time lags, which would cause the CSD indicators to begin to rise at different points in time. To avoid the risk of fine-tuning, we nevertheless make the above choice for a more conservative setting.

2.5. Deep-sea drilling core samples

CENOGRID is composed from 14 ocean drilling core records, gathered from various expeditions around the world (Westerhold et al., 2020). The data is astronomically tuned and corrected for geographic biases and offsets as thoroughly as possible. Yet, differences in sampling rates and composition between records remain. This is most notable if the CSD indicator are calculated for the whole time series with a very small window size, so that high frequencies are taken into account. This results in considerable jumps in the estimators at the exact locations where the data sources change from one core to another. Therefore, analysis of the CSD indicators is restricted to within a core. Similarly, it would be preferable if the global significance test could be done within the same drilling core where CSD occurs, since it is probable that the correlation structure is at least similar. This is however not possible, since many core records are too short to be covered by multiple independent intervals (of similar size as the trend estimation intervals prior to the events). The global test has therefore been done across core transitions to ensure a sufficient amount of independent data contributing to the global test. This should not introduce a bias however, since core changes are just as likely to produce a spurious significant trend as spoiling true trends.

There are two special influences of core changes that have to be mentioned. The Late Miocene Carbon Isotope Shift occurs at 7.6 Ma, with a core cut occurring at 8.27 Ma. This interval is too short to be analysed for CSD, so the previous core is investigated. This means that the CSD indicators could not be calculated up to the event but only up to the point where the next core starts at 8.27 Ma, which might lead to a weaker CSD signal since changes in σ and α_1 should be most pronounced just before the transition. The other situation occurs for the Tortonian Thermal Maximum. To include a sufficient amount of data in this low-resolution interval, some data is included from the drilling core preceding the one containing the event. We have ensured that this leads to no false positive trend in the CSD indicators. The preceding core has a larger autocorrelation and standard deviation than the main core. Inclusion of this data can therefore only reduce the magnitude of the trend, which could only lead to an underestimation of the significance not an overestimation. Detailed information about the exact timing of the events and analysed intervals can be found in the Supplementary Material (Table 5). It is important to note that the timing of the events is chosen to coincide with the most likely occurrence of the dynamical transition and deviate slightly from the one commonly found in the literature.

3. Results

3.1. Section I

Within the early Section part of the record we consider two major events, the Latest Danian Event and the Paleocene/Eocene Thermal Maximum (PETM). The temporal resolution of this Section of CENOGRID is 5 ka. Since trends in the time series will bias the CSD indicators, both time series are detrended using a running window filter with a centred Gaussian kernel with $s_d = 200$ ka and a bandwidth of $6s_d$. From the detrended data, the windowed standard deviation and lag-one autocorrelation are calculated using a running window width of 755 ka, where missing values are ignored (see Methods section).

The local significance test (Table 2) yields a significant increase

for seven out of the eight tested quantities prior to the events (2 events × 2 CSD indicators × 2 records). In the $\delta^{13}C$ time series, increases are found in σ and α_1 for both events. For $\delta^{18}O$ increases can be found for σ and α_1 simultaneously prior to the Latest Danian Event. The PETM is only preceded by an increase in α_1 with σ decreasing (see Supplementary Material, fig. A.5). Thus, according to our classification (Table 1), the latest Danian event exhibits synchronized CSD-like behaviour, while the PETM displays CSD-like behaviour in $\delta^{13}C$ and nondescript behaviour in $\delta^{18}O$. The global test (Table 3) indicated that the number of increases in lag-one autocorrelation before the events is significant in both records, but the only trustworthy sign for critical slowing down is an increase in α_1 and σ simultaneously. Under this criterion, the estimators are significant in the $\delta^{13}C$ time series, but not so in the $\delta^{18}O$ (due to the decrease in σ). For the same reason, the synchronized CSD-like behaviour is also not deemed globally significant according to the global test. Yet, it seems disingenuous to reject global significance of synchronized CSD due to the failure of only one out of eight quantities, since an increase in σ may be masked by independent changes in the high-frequency variability, despite CSD occurring. Because synchronized CSD-like behaviour is subject to the strictest conditions but also the strongest sign for true CSD, a moderation of these conditions is made to construct an additional global test for *partially synchronized CSD-like behaviour*. In this version of the test, findings from random sampling are considered significant if an increase in both indicators can be found in one of the two records, indicating CSD-like behaviour, with a simultaneous increase in at least one indicator in the other record. Under this test, the partially synchronized CSD-like behaviour is deemed globally significant (see Table 3). Of course, this statement is weaker than for fully synchronized EWS. Nevertheless, we chose to perform this test to check whether the strongest observable CSD indication prior to both events as an ensemble happens to be globally significant. In this case this indication is categorized as partially synchronized CSD-like behaviour which still provides stronger evidence for bifurcation-induced transitions than CSD-like behaviour in only one of the records.

3.2. Section II

The middle Section spans the interval 44–34 Ma. In this part of CENOGRID, the data points are equally spaced with an interval of 5 ka. Although this sampling rate is the same as for Section I, a much larger amount of the data is interpolated due to low data density (see Fig. 1), which demands a separate analysis. Hence, analysing of the Late Lutetian Thermal Maximum (41.5 Ma) and Middle Eocene Climate Optimum (40 Ma) is difficult. In the time leading up to these events the point density and pair density are consistently below 40% and 10%, respectively. This makes standard deviation calculations very uncertain and lag-one autocorrelation estimates impossible. Due to these limitations, analysis of CSD prior to both events is unfortunately out of question.

The Eocene/Oligocene Transition is preceded by an interval where more than ~80% of the data are missing per window (see Supplementary Material, figs. A.4 and A.6). This makes it impossible to estimate the CSD indicators on time scales similar to the previous analyses. It is only possible to examine a time frame of 0.9 Ma prior to a drill core change just before the transition, where the data has an acceptable point density of ~ 60%. The detrending Gaussian Kernel ($s_d = 0.2$) has the same width like in the early Section. The window size for the CSD indicators is now 455 ka, half of the size of the analysed time interval prior to the Eocene/Oligocene Transition.

Under these circumstances, the standard deviation increases insignificantly in the $\delta^{18}O$ record and decreases in the $\delta^{13}C$. Evaluation of α_1 yields a significant increase of the lag-one autocorrelation in both records. In any case, an increase in only α_1 and not σ can not be seen as a reliable sign of CSD. The behaviour must thus be considered nondescript. Furthermore, the limited amount of data makes a global test impossible.

3.3. Section III

The late Section covers the 34–0 Ma interval at a temporal resolution of 2 ka. Four events manifest in both time series, the Oligocene/Miocene Transition, the middle Miocene Climate Transition, the Tortonian Thermal Maximum and the Late Miocene Carbon Isotope Shift, with the Late Miocene Carbon Isotope Shift only occurring in the $\delta^{13}C$ records. Like in the previous case, we tried to find parameters that describe all events simultaneously. The detrending Gaussian Kernel is initialized with $s_d = 120$ ka a bandwidth of 720ka, the CSD estimator window has a width of 330 ka. With these parameters, CSD-like behaviour can be seen on time intervals ~2 Ma prior to all events.

The local significance test (Table 2) yields positive results for 11 out of 16 times (4 events × 2 CSD indicators × 2 records). In detail, the results show that prior to the Oligocene/Miocene Transition and the Tortonian Thermal Maximum, synchronized CSD-like behaviour is observed. The Late Miocene Carbon Isotope Shift is especially pronounced in the $\delta^{13}C$ record and significant increases can be observed here in both indicators. In the $\delta^{18}O$ time series the observed increases in standard deviation and lag-one autocorrelation is not significant, which is expected since no shift is noticeable in this record. The other three quantities without significant positive trends are all prior to the middle Miocene Climate Transition. That means no significant increases of σ or α_1 could be found here in $\delta^{18}O$ and only α_1 increases significantly in $\delta^{13}C$. This may mean that this event is not preceded by CSD, but could also be a reflection of limited data availability. Just prior to the event a drilling core change is located, which leads to a shorter time interval where CSD could be analysed. Since different records may contain

Table 3
Results of Section I global test based on 10,000 random shufflings of two points (corresponding to number of CSD candidates found in this Section). Results of local tests are compared against general behaviour of time series for nondescript, CSD-like and synchronized CSD-like null assumptions (see Methods). A significance threshold is defined at the 95th percentile of randomly observed (locally) significant positive trends. Based on local test findings, an additional category (partially synchronized CSD-like) is introduced, showing CSD-like behaviour in one time series and at least one positive trend in the other time series. Significant results are marked **bold**.

	$\delta^{13}C$		$\delta^{18}O$	
	observed	significance threshold	observed	significance threshold
σ	2	2	1	1
α_1	**2**	1	**2**	1
σ and α_1 (CSD-like)	**2**	1	1	1
	observed		significance threshold	
synchronized CSD-like	1		1	
partially synchronized	**2**		1	

different autocorrelation and standard deviation structures, analysis cannot be performed across cores as this could lead to spurious results. Additionally, the data density in the preceding core is very low, with a pair density approaching zero (see Methods section and Fig. 3). Nevertheless, the middle Miocene Climate Transition must be categorized as exhibiting nondescript behaviour and is thus not included in the global test.

For the global test (Table 4), some details have to be mentioned here. First, the period 20–15.56 Ma (a single core record) has to be excluded due to the sampling issues, with very low point and pair densities (see Methods section and Fig. 3). As mentioned, no significant signs for CSD are observed prior to the middle Miocene Climate Transition and in δ^{18}O ahead of the Late Miocene Carbon Isotope Shift. Consequently, the δ^{18}O data is analysed for two events, the Oligocene/Miocene Transition and Tortonian Thermal Maximum. The δ^{13}C time series is evaluated for three events in this part, with addition of the Late Miocene Carbon Isotope Shift. For the test where both estimators have to appear simultaneously across both available records, marking synchronized CSD-like behaviour, only the two events preceded by locally significant EWS (Oligocene/Miocene Transition, Tortonian Thermal Maximum) are used. The manifestation of synchronized CSD-like behaviour prior to both events is significant according to the global test. According to the global test, the number of CSD-like events prior to events is significant in the δ^{13}C and δ^{18}O time series independently, implying that CSD-like behaviour prior to the Late Miocene Carbon Isotope Shift is globally significant in the δ^{13}C record.

4. Discussion and conclusion

The fingerprints of critical slowing down can consistently be identified preceding some of the most prominent climate events in the Cenozoic Era, with the local and global significance tests working complementary in establishing confidence to this claim. The consistent appearance of local CSD-like behaviour (positive trends in σ and α_1) preceding events in Section I and Section III hints at bifurcations in the underlying climatic mechanism to trigger transitions. The results for the PETM (which was identified in (Westerhold et al., 2020) as the transition between warm- and hothouse state) in particular match a detailed analysis for this event and with a different dataset by Armstrong et al. (Armstrong McKay and Lenton, 2018) which lends further credibility to these results. Our global significance test confirms that the observed numbers of CSD instances are unlikely ($p < 0.05$) to occur prior to random points of the time series rather than prior to abrupt events. The revealed indications of CSD provide evidence that bifurcations are a dominant variability mode during Cenozoic Era. Especially interesting is the consistency in lead time of the occurrence of EWS for events within Section III. From our analysis, the Latest Danian Event, Oligocene/Miocene Transition and Tortonian Thermal Maximum can be considered strong candidates for bifurcation-induced transitions due to their synchronized CSD-like signals. The Paleocene/Eocene Thermal Maximum and Late Miocene Carbon Isotope Shift are candidates with CSD-like behaviour in the carbon time series. We want to stress however that this binary classification is based on a somewhat arbitrarily chosen threshold value of 0.05 for the local significance test. The Oligocene/Miocene Transition for example borders on non-significance in one quantity (0.049), while the Late Miocene Carbon Isotope Shift borders on significance (0.055) in another quantity (see Table 2). Follow-up studies will be needed to confirm that the observed signals are indeed consistent with bifurcation-induced transitions. The globally-integrated nature of CENOGRID makes it difficult to link the signs of CSD to specific physical mechanisms in the climate system. Additional information from geological data, further (regional) paleoclimate records (that may be analysed in the time and depth domain) and physical modeling is required to constrain the likely physical mechanisms behind the individual transitions. Depending on the hypothesis for the transition mechanism, concrete physical variables will have to be identified that are directly

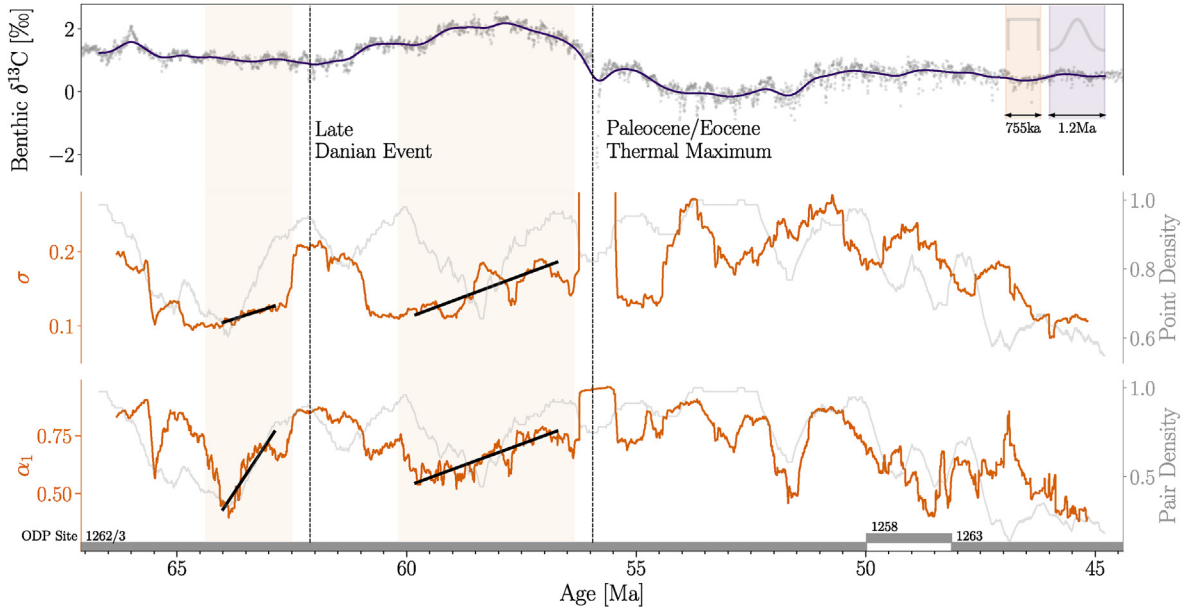

Fig. 2. Section I of the binned CENOGRID δ^{13}C time series with Gaussian-smoothed version (violet) used for detrending. CSD indicators, i.e., standard deviation σ and lag-one autocorrelation α_1, are calculated in running windows (orange). Window sizes for Gaussian detrending and CSD indicator estimation are shown in the upper right, and events are marked by vertical lines. Intervals for trend estimation (light orange) are chosen in such a way that no information about the events enters the calculation. Linear trend (black) is estimated by least squares regression; significant positive trends are marked in by solid line and non-significant trends by dashed line. Point and pair densities (grey) are calculated in the same windows as the σ and α_1 estimators. Drilling core records are indicated on the time axis (grey bands), with associated ODP Site numbers. (For interpretation of the references to colour in this figure legend, the reader is referred to the Web version of this article.)

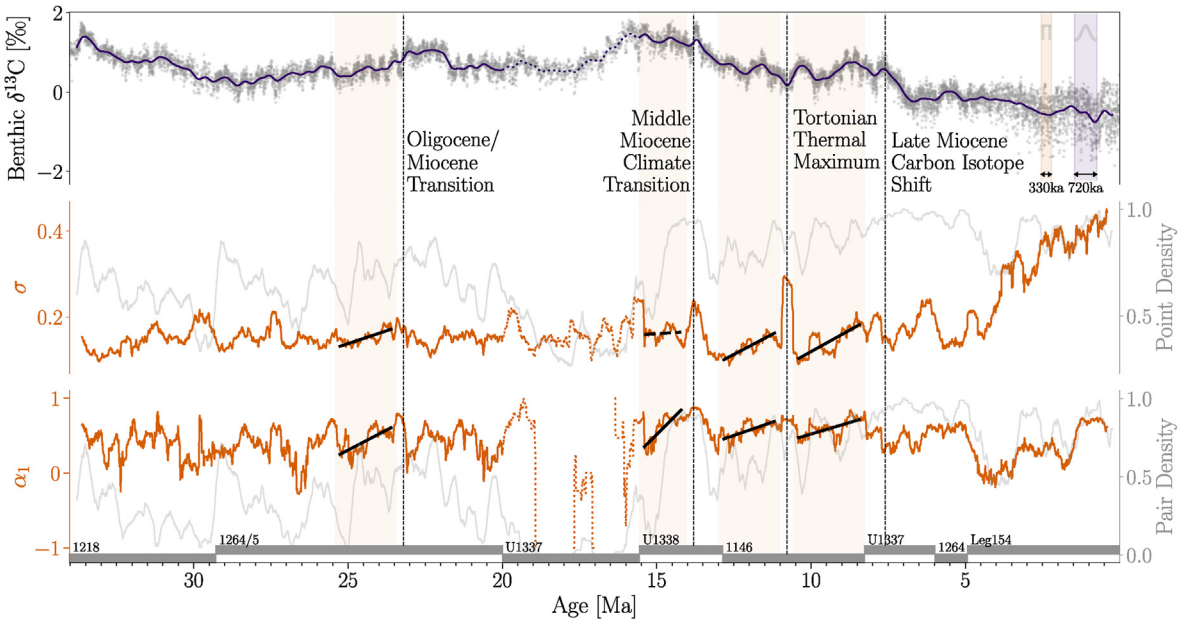

Fig. 3. Section III version (δ^{13}C) of Fig. 2. The interval 20 to 15 Ma (dotted) is excluded for the global significance test due to low data density.

Table 4
Results of Section III global test based on 10,000 random shuffling of two points (corresponding to number of CSD candidates found in this Section). Results of local tests are compared against general behaviour of time series for nondescript, CSD-like and synchronized CSD-like null assumptions (see Methods). Significant results are marked **bold**.

	δ^{13}C		δ^{18}O	
	observed	significance threshold	observed	significance threshold
σ	**3**	2	2	2
α_1	**3**	2	**2**	1
σ and α_1 (CSD-like)	**3**	1	**2**	1
	observed		significance threshold	
synchronized CSD-like	**2**		1	

linked to the transition mechanism and localized records are to be analysed for bifurcation-related behaviour.

As mentioned in the methods section, one may criticize that the CSD analysis intervals and lead times are chosen freely. This is a general issue in the analysis of EWS in empirical time series. To identify relevant time scales beforehand, information about the basin of attraction and noise properties would be needed. Without an underlying physical model it is difficult to establish a univocal proof that the studied events are caused by bifurcations and the observed features are in fact manifestations of critical slowing down. Nonetheless, the results gain credibility through the strong synchronisation of CSD signals not only within, but also across both records.

One of the most intriguing transitions in the Cenozoic is certainly the transition between Green- and icehouse climate state, the Eocene/Oligocene Transition (EOT). Woefully, this is a time span of low data density in CENOGRID, so that only a weak statement can be made about the occurrence of CSD for this event. While (locally) significant increases in the lag-one autocorrelation can be found before this transition, the standard deviation is showing no significant increase in both records. Since CSD demands an increase in both indicators, we cannot declare this event to exhibit CSD-like behaviour. At the same time, this result is not comparable in terms of reliability to those received for Section I and III events due to the lack of data. More complete records for the time period 40–33 Ma are required to make a more definite statement. A similar analysis of a $CaCO_3$ sample by Dakos et al. (2008) indicates an increase of lag-one autocorrelation prior to the EOT, starting at 40 Ma. While this would strengthen the result presented here, an independent analysis of this data (Tripati et al., 2005) yields problems. For one, $CaCO_3$ data only exhibits an increase in autocorrelation, but a decrease in the standard deviation, similar to our result for the CENOGRID records. As argued before, both of the indicators have to show a significant increase to be an acceptable sign of CSD (Ditlevsen and Johnsen, 1944-8007). Even more concerning is the fact that the $CaCO_3$ time series shows a consistent decrease of the data density leading up to the event. The previous analysis deals with this problem by interpolating the dataset (Dakos et al., 2008), a procedure that can lead to spurious increases in the autocorrelation as argued before (see Methods section). This could lead to a false positive confirmation of an increase in the CSD indicators. By binning the data and re-performing our analysis, we are nonetheless able to reproduce a significant increase in autocorrelation, but also a decrease in standard deviation (see Supplementary Material, fig. A.12). This behaviour is not CSD-like, but consistent with our findings. Due to the limitations of this dataset, no global test can be performed. Ultimately, there is no compelling evidence for this transition to be bifurcation-induced based on these two datasets. In the future, additional records of this time period might be added to composite records like CENOGRID, increasing the data density, so that a more definite statement can be made.

Finally, we want to mention some limitations of the presented analysis, and propose some extensions and further research directions. The present work is suitable for assessing the hypothesis that bifurcations are a likely mechanism triggering abrupt climate events in the Cenozoic qualitatively. It can, however, not be used to quantitatively judge the probability that specific events are preceded by critical slowing down. Such an analysis requires more scrutinizing methods, physical modeling and additional paleoclimate records, which is beyond the scope of this paper (see (Armstrong McKay and Lenton, 2018) for such an analysis of the PETM and interpretations of physical mechanisms). Another omission from our analysis is the direct estimation of uncertainties for the σ and α_1 estimators and consequently of the trends. Uncertainties in the original data (e.g. due to observational variations in the isotope ratios or the astronomical tuning of the data) may influence trend estimation. While some progress has been made in assessing the propagation of such uncertainties in time series data (Goswami et al., 2018), issues remain in quantifying the original data uncertainties. This is especially true for highly processed records such as CENOGRID, due to its composite nature and astronomically tuning. The data availability fluctuations between different windows introduce another source of stochastic uncertainty. These issues have however been at least partially alleviated by the use of our local and global significance test. It can be argued that false positive results due to these effects are just as likely in any part of the records and should have thus been picked up in form of non-significant results in the global test. Variations in data availability between windows similarly influence the local test. The results can therefore be regarded as robust within the analysed dataset. To further strengthen the results, cross-analysis with alternative paleoclimate records as part of follow-up studies is advised.

In conclusion, CENOGRID provides a new opportunity for the study of tipping mechanisms in deep-time paleoclimate. The importance of critical transitions in the long-term evolution of the global climate has been recognized over the past decades. The presented work provides new evidence that bifurcations are a key mechanism for sudden changes in the global climate system, and provides a number of candidate climate events which are suited for follow-up studies.

CRediT author statement

Christopher Boettner: Writing - Original Draft, Methodology, Formal analysis, Software, Visualization. Georg Klinghammer: Writing - Original Draft, Methodology, Software, Validation. Niklas Boers: Conceptualization, Writing- Reviewing and Editing. Norbert Marwan: Conceptualization, Project administration, Writing-Reviewing and Editing. Thomas Westerhold: Writing- Reviewing and Editing.

Declaration of competing interest

The authors declare that they have no known competing financial interests or personal relationships that could have appeared to influence the work reported in this paper.

Appendix A. Supplementary data

Supplementary data to this article can be found online at https://doi.org/10.1016/j.quascirev.2021.107177.

References

Adams, J., Maslin, M., Thomas, E., 1999. Sudden climate transitions during the quaternary. Prog. Phys. Geogr.: Earth Environ. 23 (1), 1–36. https://doi.org/10.1177/030913339902300101. ISSN 0309-1333, 1477-0296.

Alley, R.B., Marotzke, J., Nordhaus, W.D., Overpeck, J.T., Peteet, D.M., Pielke, R.A., Pierrehumbert, R.T., Rhines, P.B., Stocker, T.F., Talley, L.D., Wallace, J.M., 2003. Abrupt climate change. Science 299 (5615), 2005–2010. https://doi.org/10.1126/science.1081056. ISSN 0036-8075, 1095-9203.

Alvarez, L.W., Alvarez, W., Asaro, F., Michel, H.V., 1980. Extraterrestrial cause for the cretaceous-tertiary extinction. Science 208 (4448), 1095–1108. https://doi.org/10.1126/science.208.4448.1095. ISSN 0036-8075, 1095-9203.

Armstrong McKay, D.I., Lenton, T.M., 2018. Reduced carbon cycle resilience across the palaeocene–eocene thermal Maximum. Clim. Past 14 (10), 1515–1527. https://doi.org/10.5194/cp-14-1515-2018. ISSN 1814-9324.

Ashwin, P., Wieczorek, S., Vitolo, R., Cox, P., 1962. Tipping points in open systems: bifurcation, noise-induced and rate-dependent examples in the climate system. Phil. Trans. Math. Phys. Eng. Sci. 370 (2012), 1166–1184. https://doi.org/10.1098/rsta.2011.0306. ISSN 1364-503X, 1471-2962.

Boers, N., 2018. Early-warning signals for Dansgaard-Oeschger events in a high-resolution ice core record. Nat. Commun. 9 (1), 2556. https://doi.org/10.1038/s41467-018-04881-7. ISSN 2041-1723.

Bohaty, S.M., Zachos, J.C., 2003. Significant southern ocean warming event in the late middle Eocene. Geology 31 (11), 1017–1020. https://doi.org/10.1130/G19800.1. ISSN 0091-7613.

Bornemann, A., Schulte, P., Sprong, J., Steurbaut, E., Youssef, M., Speijer, R.P., 2009. Latest danian carbon isotope anomaly and associated environmental change in the southern tethys (nile basin, Egypt). J. Geol. Soc. 166 (6), 1135–1142. https://doi.org/10.1144/0016-76492008-104. ISSN 0016-7649, 2041-479X.

Budyko, M.I., 1969. The effect of solar radiation variations on the climate of the Earth. Tellus 21 (5), 611–619. https://doi.org/10.1111/j.2153-3490.1969.tb00466.x. ISSN 2153-3490.

Dakos, V., Scheffer, M., van Nes, E.H., Brovkin, V., Petoukhov, V., Held, H., 2008. Slowing down as an early warning signal for abrupt climate change. Proc. Natl. Acad. Sci. Unit. States Am. 105 (38), 14308–14312. https://doi.org/10.1073/pnas.0802430105. ISSN 0027-8424, 1091-6490.

Ditlevsen, P.D., Johnsen, S.J., 1944-8007. Tipping points: early warning and wishful thinking. Geophys. Res. Lett. 37 (19). https://doi.org/10.1029/2010GL044486.

Drijfhout, S., Bathiany, S., Beaulieu, C., Brovkin, V., Claussen, M., Huntingford, C., Scheffer, M., Sgubin, G., Swingedouw, D., 2015. Catalogue of abrupt shifts in intergovernmental panel on climate change climate models. Proc. Natl. Acad. Sci. Unit. States Am. 112 (43), E5777–E5786. https://doi.org/10.1073/pnas.1511451112. ISSN 0027-8424, 1091-6490.

El-Hacen, E.-H.M., Bouma, T.J., Fivash, G.S., Sall, A.A., Piersma, T., Olff, H., Govers, L.L., 2018. Evidence for 'critical slowing down' in seagrass: a stress gradient experiment at the southern limit of its range. Sci. Rep. 8 (1), 17263. https://doi.org/10.1038/s41598-018-34977-5. ISSN 2045-2322.

Goswami, B., Boers, N., Rheinwalt, A., Marwan, N., Heitzig, J., Breitenbach, S.F.M., Kurths, J., 2018. Abrupt transitions in time series with uncertainties. Nat. Commun. 9 (1), 48. https://doi.org/10.1038/s41467-017-02456-6. ISSN 2041-1723.

Hodell, D.A., Curtis, J.H., Sierro, F.J., Raymo, M.E., 2001. Correlation of late Miocene to early Pliocene sequences between the mediterranean and north atlantic. Paleoceanography 16 (2), 164–178. https://doi.org/10.1029/1999PA000487. ISSN 1944-9186.

Kleinen, T., Held, H., Petschel-Held, G., 2003. The potential role of spectral properties in detecting thresholds in the Earth system: application to the thermohaline circulation. Ocean Dynam. 53 (2), 53–63. https://doi.org/10.1007/s10236-002-0023-6. ISSN 1616-7228.

Kuehn, C., 2011. A mathematical framework for critical transitions: bifurcations, fast–slow systems and stochastic dynamics. Phys. Nonlinear Phenom. 240 (12), 1020–1035. https://doi.org/10.1016/j.physd.2011.02.012. ISSN 0167-2789.

Lancaster, G., Iatsenko, D., Pidde, A., Ticcinelli, V., Stefanovska, A., 2018. Surrogate data for hypothesis testing of physical systems. Phys. Rep. 748, 1–60. https://doi.org/10.1016/j.physrep.2018.06.001. ISSN 0370-1573.

Lenton, T.M., Schellnhuber, H.J., 2007. Tipping the scales. Nat. Clim. Change 1 (712), 97–98. https://doi.org/10.1038/climate.2007.65. ISSN 1758-6798.

Lenton, T.M., Held, H., Kriegler, E., Hall, J.W., Lucht, W., Rahmstorf, S., Schellnhuber, H.J., 2008. Tipping elements in the Earth's climate system. Proc. Natl. Acad. Sci. Unit. States Am. 105 (6), 1786–1793. https://doi.org/10.1073/pnas.0705414105. ISSN 0027-8424, 1091-6490.

Lenton, T.M., Rockström, J., Gaffney, O., Rahmstorf, S., Richardson, K., Steffen, W., Schellnhuber, H.J., 2019. Climate tipping points — too risky to bet against. Nature 575 (7784), 592–595. https://doi.org/10.1038/d41586-019-03595-0. ISSN 0028-0836, 1476-4687.

McInerney, F.A., Wing, S.L., 2011. The paleocene-eocene thermal Maximum: a perturbation of carbon cycle, climate, and biosphere with implications for the future. Annu. Rev. Earth Planet Sci. 39 (1), 489–516. https://doi.org/10.1146/annurev-earth-040610-133431.

Miller, K.G., Fairbanks, R.G., Mountain, G.S., 1987. Tertiary oxygen isotope synthesis, sea level history, and continental margin erosion. Paleoceanography 2 (1), 1–19. https://doi.org/10.1029/PA002i001p00001. ISSN 08838305.

Mudelsee, M., Bickert, T., Lear, C.H., Lohmann, G., 2014. Cenozoic climate changes: a review based on time series analysis of marine benthic d18O records. Rev. Geophys. 52 (3), 333–374. https://doi.org/10.1002/2013RG000440. ISSN 1944-9208.

Pearson, P.N., Palmer, M.R., 2000. Atmospheric carbon dioxide concentrations over the past 60 million years. Nature 406 (6797), 695–699. https://doi.org/10.1038/

35021000. ISSN 1476-4687.
Rehfeld, K., Marwan, N., Heitzig, J., Kurths, J., 2011. Comparison of correlation analysis techniques for irregularly sampled time series. Nonlinear Process Geophys. 18 (3), 389–404. https://doi.org/10.5194/npg-18-389-2011. ISSN 1023-5809.
Rypdal, M., 2015. Early-Warning Signals for the Onsets of Greenland Interstadials and the Younger Dryas-Preboreal Transition. https://doi.org/10.1175/JCLI-D-15-0828.1 arXiv:1512.07381 [physics].
Scheffer, M., Bascompte, J., Brock, W.A., Brovkin, V., Carpenter, S.R., Dakos, V., Held, H., van Nes, E.H., Rietkerk, M., Sugihara, G., 2009. Early-warning signals for critical transitions. Nature 461 (7260), 53–59. https://doi.org/10.1038/nature08227. ISSN 1476-4687.
Schulz, M., Mudelsee, M., 2002. REDFIT: estimating red-noise spectra directly from unevenly spaced paleoclimatic time series. Comput. Geosci. 28 (3), 421–426. https://doi.org/10.1016/S0098-3004(01)00044-9. ISSN 00983004.
Schulz, M., Stattegger, K., 1997. Spectrum: spectral analysis of unevenly spaced paleoclimatic time series. Comput. Geosci. 23 (9), 929–945. https://doi.org/10.1016/S0098-3004(97)00087-3. ISSN 00983004.
Sellers, W.D., 1969. A global climatic model based on the energy balance of the earth-atmosphere system. Journal of Applied Meteorology and Climatology 8 (3), 392–400. https://doi.org/10.1175/1520-0450(1969)008<0392:AGCMBO>2.0.CO;2. ISSN 1520-0450.
Steffen, W., Rockström, J., Richardson, K., Lenton, T.M., Folke, C., Liverman, D., Summerhayes, C.P., Barnosky, A.D., Cornell, S.E., Crucifix, M., Donges, J.F., Fetzer, I., Lade, S.J., Scheffer, M., Winkelmann, R., Schellnhuber, H.J., 2018. Trajectories of the Earth system in the anthropocene. Proc. Natl. Acad. Sci. Unit. States Am. 115 (33), 8252–8259. https://doi.org/10.1073/pnas.1810141115. ISSN 0027-8424, 1091-6490.
Stommel, H., 1961. Thermohaline convection with two stable regimes of flow. Tellus 13 (2), 224–230. https://doi.org/10.1111/j.2153-3490.1961.tb00079.x. ISSN 2153-3490.
Trauth, M.H., Asrat, A., Duesing, W., Foerster, V., Kraemer, K.H., Marwan, N., Maslin, M.A., Schaebitz, F., 2019. Classifying past climate change in the chew bahir basin, southern Ethiopia, using recurrence quantification analysis. Clim. Dynam. 53 (5), 2557–2572. https://doi.org/10.1007/s00382-019-04641-3. ISSN 1432-0894.
Carbon Cycle change in the Eocene, supplement to: Tripati, Aradhna K; Backman, Jan; Elderfield, Henry; Ferretti, Patrizia Tripati, A.K., Backman, J., Elderfield, H., Ferretti, P., 2005. Eocene bipolar glaciation associated with global carbon cycle changes. Nature 436, 341–346. https://doi.org/10.1594/PANGAEA.738240. PANGAEA (2005) 8 datasetsdoi.
Valdes, P., 2011. Built for stability. Nat. Geosci. 4 (7), 414–416. https://doi.org/10.1038/ngeo1200. ISSN 1752-0908.
Vettoretti, G., Peltier, W.R., 2016. Thermohaline instability and the formation of glacial north atlantic super polynyas at the onset of Dansgaard-Oeschger warming events. Geophys. Res. Lett. 43 (10), 5336–5344. https://doi.org/10.1002/2016GL068891. ISSN 1944-8007.
Westerhold, T., Röhl, U., Donner, B., McCarren, H.K., Zachos, J.C., 2011. A complete high-resolution Paleocene benthic stable isotope record for the central pacific (ODP site 1209). Paleoceanography 26 (2), 1944–9186. https://doi.org/10.1029/2010PA002092.
Westerhold, T., Röhl, U., Donner, B., Frederichs, T., Kordesch, W.E.C., Bohaty, S.M., Hodell, D.A., Laskar, J., Zeebe, R.E., 2018. Late lutetian thermal maximum—crossing a thermal threshold in Earth's climate system? G-cubed 19 (1), 73–82. https://doi.org/10.1002/2017GC007240. ISSN 1525-2027.
Westerhold, T., Marwan, N., Drury, A.J., Liebrand, D., Agnini, C., Anagnostou, E., Barnet, J.S.K., Bohaty, S.M., Vleeschouwer, D.D., Florindo, F., Frederichs, T., Hodell, D.A., Holbourn, A.E., Kroon, D., Lauretano, V., Littler, K., Lourens, L.J., Lyle, M., Pälike, H., Röhl, U., Tian, J., Wilkens, R.H., Wilson, P.A., Zachos, J.C., 2020. An astronomically dated record of Earth's climate and its predictability over the last 66 million years. Science 369 (6509), 1383–1387. https://doi.org/10.1126/science.aba6853. ISSN 0036-8075, 1095-9203.
Xu, C., Kohler, T.A., Lenton, T.M., Svenning, J.-C., Scheffer, M., 2020. Future of the human climate niche. Proc. Natl. Acad. Sci. Unit. States Am. 117 (21), 11350–11355. https://doi.org/10.1073/pnas.1910114117. ISSN 0027-8424, 1091-6490.
Zachos, J.C., Lohmann, K.C., Walker, J.C., Wise, S.W., 1993. Abrupt climate change and transient climates during the paleogene: a marine perspective. J. Geol. 101 (2), 191–213. https://doi.org/10.1086/648216. ISSN 0022-1376.
Zachos, J.C., Flower, B.P., Paul, H., 1997. Orbitally paced climate oscillations across the oligocene/miocene boundary. Nature 388 (6642), 567–570. https://doi.org/10.1038/41528. ISSN 1476-4687.